

Article

Tannic Acid Coatings to Control the Degradation of AZ91 Mg Alloy Porous Structures

Silvia Spriano ^{1,*}, Anna Dmitruk ², Krzysztof Naplocha ² and Sara Ferraris ¹¹ Politecnico di Torino, Department of Applied Science and Technology, 10129 Torino, Italy² Department of Lightweight Elements Engineering, Foundry and Automation, Faculty of Mechanical Engineering, Wrocław University of Science and Technology, Wybrzeże Wyspińskiego 27, 50-370 Wrocław, Poland* Correspondence: silvia.spriano@polito.it; Tel.: +39-0110905768

Abstract: Porous structures of magnesium alloys are promising bioimplants due to their biocompatibility and biodegradability. However, their degradation is too rapid compared to tissue regeneration and does not allow a progressive metal substitution with the new biological tissue. Moreover, rapid degradation is connected to an accelerated ion release, hydrogen development, and pH increase, which are often causes of tissue inflammation. In the present research, a natural organic coating based on tannic acid was obtained on Mg AZ91 porous structures without toxic reagents. Mg AZ91 porous structures have been prepared by the innovative combination of 3D printing and investment casting, allowing fully customized objects to be produced. Bare and coated samples were characterized using scanning electron microscopy equipped with energy dispersive spectroscopy (SEM-EDS), fluorescence microscopy, Fourier transformed infrared spectroscopy (FTIR), tape adhesion test, Folin-Ciocalteu, and degradation tests. Different parameters (solvent, dipping time) were compared to optimize the coating process. The optimized coating was uniform on the outer and inner surfaces of the porous structures and significantly reduced the material degradation rate and pH increase in physiological conditions (phosphate-buffered saline—PBS).

Keywords: magnesium; tannic acid; degradation; coating; biodegradability

Citation: Spriano, S.; Dmitruk, A.; Naplocha, K.; Ferraris, S. Tannic Acid Coatings to Control the Degradation of AZ91 Mg Alloy Porous Structures. *Metals* **2023**, *13*, 200. <https://doi.org/10.3390/met13020200>

Academic Editors: Crtomir Donik and Irena Paulin

Received: 7 December 2022

Revised: 30 December 2022

Accepted: 15 January 2023

Published: 19 January 2023



Copyright: © 2023 by the authors. Licensee MDPI, Basel, Switzerland. This article is an open access article distributed under the terms and conditions of the Creative Commons Attribution (CC BY) license (<https://creativecommons.org/licenses/by/4.0/>).

1. Introduction

Magnesium and its alloys are receiving interest as possible materials for degradable implants. Magnesium is a biodegradable and biocompatible metal; it is involved in numerous biochemical reactions in the human body, such as bone regeneration and cardiovascular protection [1]. Moreover, one anti-inflammatory effect of Mg²⁺ ions was reported as the ability to promote the M2 polarization of macrophages [1,2]. Furthermore, magnesium and its alloys have an elastic modulus (41–45 GPa) closer to one of the human bones than stainless steel and titanium, being suitable for avoiding stress shielding phenomena [1,3]. Moreover, Mg²⁺ ions are involved in osteogenic differentiation, angiogenesis, limitation of osteoclastogenesis, and improvement of hydroxyapatite properties (substituting Ca²⁺ ions) [1], making them promising candidates for bone contact applications, especially temporary ones. Biodegradable metals are also of interest for cardiovascular stents, where prosthesis support is required for the time needed for arterial remodeling (typically 6–12 months) [4]. No significant benefit can be obtained after this period, but some complications can occur (e.g., long-term endothelial dysfunction, delayed re-endothelialization, thrombogenicity, permanent physical irritation, chronic inflammatory local reactions), making the development of suitable degradable stents particularly interesting [4].

For orthopedic and cardiovascular applications, the main limitations to the diffusion of magnesium-based degradable implants are too fast degradation combined with hydrogen gas development and significant pH increase, which cause the premature loss of mechanical requirements. In addition, some inflammatory and potentially dangerous biological effects

are connected to fast degradation [1,3,4]. Mg^{2+} ions enrich the intracellular content by being renally controlled, as shown in the case of the oral administration of magnesium. On the other side, biodegradation of magnesium implants produces various decomposition products (Mg^{2+} ions, hydroxides, oxides, chlorides, Mg-containing hydroxyapatite, hydrogen gas, and OH^-) and they are generally not regulated by systemic renal control [5]. These products can positively affect tissue metabolism reasonably, but a burst and intense release can represent an issue.

Several solutions have been proposed in the scientific literature to overcome the problem of too-fast degradation. While heat treatments, micro-alloying, and plastic deformation modify the alloy microstructure and, consequently, its mechanical properties [6], surface modifications, and coatings seem the most promising strategies because they affect only surface properties and do not alter the mechanical ones. Among surface modifications, conversion and deposition coatings are the most studied. Conversion coatings are in situ grown coatings, which derive from specific reactions (chemical reactions of dissolution/deposition, anodization, plasma electrolytic oxidation (PEO), and alkali-heat treatments) on the material surface and the consequent development of a coating. Phosphates and oxides are the most diffused conversion coatings on Mg alloys [6,7]. Deposition of the coatings can be obtained using physical vapor deposition (PVD), atomic layer deposition (ALD), electrolytic deposition, sol-gel, and dip coating. Both inorganic (e.g., hydroxyapatite, diamond-like carbon, SiO_2 , and TiO_2) and organic (polylactic acid—PLA, polylactic-co-glycolic acid—PLGA, polycaprolactone—PLC, and stearic acid—SA) coatings have been proposed for the degradation control of magnesium and its alloys [6,7]. Multifunctional properties of these coatings (e.g., osteointegration or drug loading abilities) can increase their potential, but a coating suitable to meet the medical needs is still far to be developed.

Polyphenols are natural molecules of vegetal origin widely studied for their numerous beneficial properties, such as the antioxidant, anti-inflammatory, antibacterial, anticancer, bone stimulating, and vasculoprotective ones, and are gaining increasing interest in industrial and medical applications [8,9]. Moreover, the corrosion protection abilities of polyphenols on metallic surfaces have been evidenced [10,11].

The possibility of exploiting the corrosion protection properties of polyphenols in the degradation control of magnesium alloys was recently explored in the scientific literature. Some works report the use of tannic acid [12,13], epigallocatechin gallate [14–16], and gallic acid [16,17] for the obtainment of organic coatings on magnesium alloys for degradation control. Polyphenols were dissolved in water, and the majority of the coatings were produced by dip coating with one [13,16,18] or more immersions (layer-by-layer approach) [12,14,15] in the polyphenolic solution. A pre-oxidation treatment using immersion in NaOH [11] or micro-arc oxidation (MAO) [16] has been proposed in some cases to improve the substrate affinity for grafting. Moreover, some authors suggested the use of hexamethylenediamine [17] or polyethyleneimine (PEI) [15] to improve the bonding ability and stability of the coating, but the biocompatibility of these molecules is low. Finally, some authors [12,14] suggest the addition of magnesium ions to the solution of polyphenols for forming metal-phenol complexes useful for coating formation and adhesion.

Three-dimensional porous structures have been selected because of their interesting clinical applications and because they maximize the degradation issue due to the large-exposed surface area. The hereby proposed cellular structures, cast from magnesium alloy, possessed orifices aiming the intensified tissue ingrowth. The honeycomb structure is light, stiff, and can be easily tailored. The foreseen application is focused on customized biodegradable magnesium-based implants (such as bone substitutes) with mechanical properties comparable to the natural bone that will be characterized by spatial structures beneficial for osseointegration and covered with protective coatings enhancing corrosion resistance and prolonging the bio-resorption time. Moreover, the production process of these structures (combination of 3D printing–fused deposition modeling, FDM, and investment casting) constitutes an innovative process. A certain innovation ensured by such an approach relates to the ease of customization of the implant's shape. The technology is

very flexible; nearly any kind of polymer pattern can be produced and replaced precisely by a chosen metal. In addition, the FDM method for pattern creation results in layered texture on the element's surface, which is then transferred to the metal part. This effect may positively affect the tissue ingrowth and adhesion at the interface of magnesium casting and the deposited coating.

In the present research work, tannic acid coatings on AZ91 Mg alloy-porous structures were obtained from water-based solutions (water or phosphate-buffered saline—PBS) in a single passage without the addition of any spacer, salt, or toxic reagent. Moreover, the coating was obtained on as-prepared (only washed) substrates without pre-oxidation treatment. Compared to the strategies proposed in the literature, the method presented here is faster (single passage, no pre-treatment of the substrates), more sustainable (no employment of toxic substances), and cheaper (reduction of process time and reagents consumption). Furthermore, tannic acid–Mg complexes were formed by exploiting the magnesium release in the coating medium without adding magnesium salts. Lastly, acid tannic is known for its anti-bacterial and antioxidant action, and this coating has potential multifunctional abilities. Surfaces were characterized using scanning electron microscopy equipped with energy dispersive spectroscopy (SEM-EDS), Fourier transformed infrared spectroscopy (FTIR), tape adhesion test, fluorescence microscopy, Folin–Ciocalteu redox activity test, and degradation tests in PBS.

2. Materials and Methods

2.1. Samples Preparation

Samples were manufactured using two combined technologies: 3D printing (fused deposition modeling, FDM) and investment casting. Firstly, additive manufacturing from polylactide (PLA) produced the exact polymer patterns for casting. Honeycomb perforated models were designed in Autodesk Inventor Professional 2018 software, and on their basis, the G-code files were created in the PrusaSlicer program. Next, spatial biomimetic PLA samples were produced using a Prusa I3-MK3S 3D printer. The patterns were fabricated in three types: 2 bigger ones (approximately 20 mm in diameter, 30 mm in height) with differing perforations of Φ 1.5 or 3 mm and one smaller (approximately 10 mm in diameter, 10 mm in height with orifices of Φ 1 mm).

Wall thickness in each case was equal to 0.6 mm. Thus, prepared polymer models were firstly attached to the wax gating system, mounted in the casting flasks, and flooded with a casting plaster water solution (Ransom & Randolph Argentum). After solidification of the ceramic molds, they were subjected to the burn-out cycle with a maximum temperature of 730 °C, which enabled the full dehydration, hardening of the plate, and complete gasification of both the wax and polymer parts of the pattern, and then cooled down to the pouring temperature of 550–600 °C. The AZ91 magnesium casting alloy (9 wt.% of Al, 0.13 wt.% of Mn, and 0.7 wt.% of Zn, rest Mg) was utilized to fill the mold cavities reflecting the shape of the models. This alloy is characterized by high castability and good mechanical properties. The developed process and parameters limit the exothermic reaction of liquid magnesium with oxygen and the local temperature increase. If the temperature rises over about 1300 °C, the component of the molding sand (CaSO_4) may decompose, releasing oxygen, which will begin to react intensively with magnesium even under a tight gas shield (SF_6). In the last step, the castings were washed after solidification, and the gypsum remnants were removed. Samples of different dimensions have been produced by this route, and some examples are shown in Figure 1a.

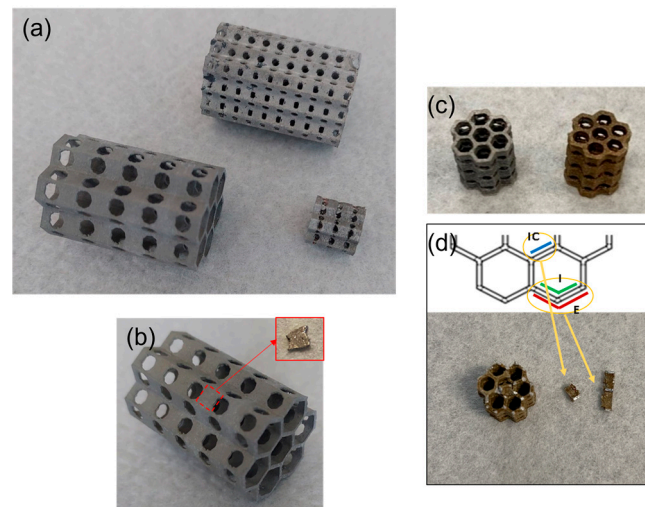


Figure 1. (a) AZ91 porous structures, (b) cutting of plane samples for the optimization of the coating and surface characterization, (c) small porous structure before (on the left) and after (on the right) the tannic acid coating, (d) cutting of samples from the coated 3D structures for the evaluation of homogeneity.

2.2. Tannic Acid Coatings

Tannic acid (TA, Tannic Acid 403040-100G Sigma Aldrich, St. Louis, MO, USA) was dissolved in ultrapure water or phosphate-buffered saline (PBS, phosphate-buffered saline 79382-50TAB Sigma Aldrich) to obtain coating solutions with different pH and ionic compositions.

Small AZ91 samples were obtained from porous structures, as shown in Figure 1b, for the optimization of the coating and surface characterization. Samples were washed in ethanol (5 min in an ultrasonic bath) and ultrapure water (5 min in an ultrasonic bath) and let dry in the air.

Washed samples were immersed in the water/PBS-based solutions of tannic acid (5 ml for each sample, with a total external surface area of approximately 0.51 cm²) for 15–30 min, 1 h, and 3 h at 37 °C. At the end of the dipping, the samples were gently washed in ultrapure water and let dry in the air.

The 3D samples (9.7 mm main dimension of the hexagonal base and 9.9 mm height, as shown in Figure 1c) were coated with the optimized conditions, defined on small plane samples, to test the feasibility of the procedure applied to complex 3D porous structures and to obtain a homogeneous coating.

2.3. Mechanical Characterizations

The cast samples were subjected to compression tests using the universal testing machine Tinius Olsen H25KT with a test speed of 5 mm/min and a maximum load of 10 kN.

The adhesion of the tannic acid coating was evaluated using the tape adhesion test performed according to the ASTM D 3359 standard [19]. However, due to the low thickness of the coating and the roughness of the substrate, the test was performed without the grid only by tape application and removal.

2.4. Surface Characterization

Surface morphology and semi-quantitative chemical composition were investigated using scanning electron microscopy equipped with energy dispersive spectroscopy (SEM, JEOL, JCM 6000 plus, EDS, JEOL, and JED 2300).

Before and after tape adhesion tests, the presence of tannic acid on AZ91 surfaces was verified using the Fourier transformed infrared spectroscopy in attenuated total reflectance mode (FTIR-ATR, Nicolet iS50 FTIR Spectrometer, Thermo Scientific, Waltham, MA, USA).

The presence and distribution of tannic acid on the surface of the samples were investigated using Fluorescence Microscopy. A confocal microscope (LSM 900, ZEISS)

equipped with a fluorescent light source (excitation wavelength 573 nm) was used for this purpose exploiting the polyphenols autofluorescence reported in the literature [20,21] and previously observed by the authors [22].

The presence and redox activity of tannic acid on the functionalized samples were analyzed using the Folin–Ciocalteu test, optimized by the authors for the analysis of solid samples [23]. Briefly, each sample was immersed in 8 ml of ultrapure water, then 0.5 ml of the Folin–Ciocalteu reagent (Folin–Ciocalteu phenol reagent 2 M, 47641-500ML-F Sigma Aldrich) and 1.5 ml of 20% *w/v* Na₂CO₃ were added and the absorbance of the solution at 760 nm recorded after 2 h and compared with the standard curve performed with gallic acid.

Degradation studies were performed according to the ASTM G31-72 standard [24]. Briefly, each sample (with a total external surface area of approximately 0.51 cm²) was soaked in 20 ml of PBS to follow the suggestion of the standard test to have a ratio between the volume of the solution (V_{sol}) and the external surface of the sample (S_s) higher than 30 ml/cm² ($V_{sol}/S_s \geq 30$ ml/cm²). Samples were soaked for different experimental times, up to 14 days (1, 2, 7, 14 days), and the solution was refreshed every 3 days. After immersion, samples were visually inspected, weighted to evaluate the weight loss/gain, and analyzed by SEM-EDS to monitor the surface chemical analysis. As far as the soaking solutions are concerned, pH measurements were performed to monitor the ability of a coating to control the degradation and consequent pH rise. In addition, the Mg concentration in the soaking solutions was measured using a portable photometer specific for Mg and Ca ions (Calcium and Magnesium Photometer HI97752, Hanna Instruments, Woonsocket, RI, USA). Finally, the presence of tannic acid in the soaking solutions was investigated using UV-Vis Spectroscopy (Shimadzu UV2600).

All the surface characterizations were performed on small planar samples cut from the 3D structures. To verify the homogeneity of the coating on 3D porous structures, small specimens were obtained from the functionalized structure in different zones, as shown in Figure 1d.

3. Results and Discussion

The compression strength was measured to ensure the repeatability of the mechanical properties of the 3D porous structures. AZ91 honeycombs, with Φ 1.5 mm orifices and cells of 3.5 mm, exhibited twofold higher strength during a quasi-static test, expressed by the plateau range in the stress–strain curve than observed for the other ones (orifices— Φ 3 mm, cells—6 mm). The forces recorded during compression at this stage were approximately 4 and 2 kN, respectively.

The tannic acid coating visually alters the color of the AZ91 surfaces, which move from bright grey to brownish, as shown in Figures 1c, 2 and 3 for the 3D construct and small samples (prepared in different conditions of coating), respectively. However, no weight loss was noticed during the coating procedure, suggesting no alteration of the alloy during the process.

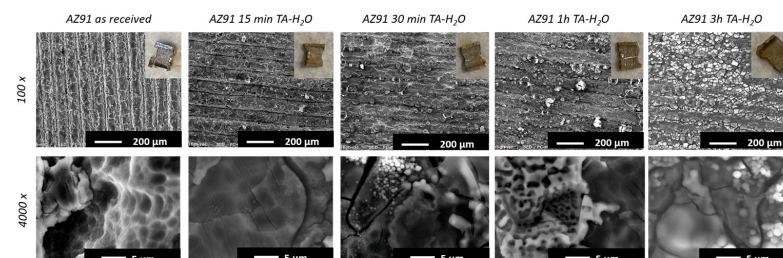


Figure 2. SEM and macro images of AZ91 samples before and after the TA coating in a water solution for different dipping times.

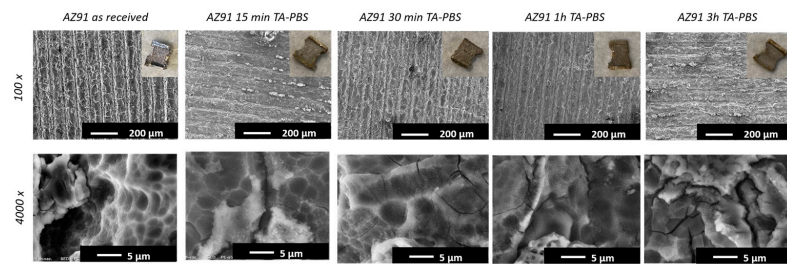


Figure 3. SEM and macro images of AZ91 samples before and after the TA coating in a PBS solution for different dipping times.

Figures 2 and 3 show the surface morphology of AZ91 samples before and after the TA coating. It can be observed that the grooved morphology (characteristic of the as-received samples) is maintained after the coating in all conditions. Such developed texture with an enlarged specific surface area is a direct result of the chosen manufacturing technology—deposition of PLA material in a layer-by-layer way during 3D printing. It may be beneficial for the ingrowth of biological tissue. This observation suggests the presence of a thin coating able to preserve the starting surface micro-texture and that no significant surface degradation/corrosion occurs during the coating process. The maintenance of the surface topography suggests a submicrometric thickness of the tannic acid coating.

The micro-scale appearance of the samples coated with tannic acid in water evidences a smoother morphology compared to the ones coated in PBS, suggesting the presence of a more homogeneous surface layer, as confirmed by EDS analyses in the following. Moreover, small precipitates and flakes are visible on the coatings obtained in water TA solution for over 30 min. They can be attributed to a more pronounced reaction of the metal in the coating solution and a greater presence of tannic acid on the surface.

Figure 4 plots the carbon content on the surface of the as-received and TA-coated, in different conditions, AZ91 samples. The TA coating induces an increase in the carbon content (from 7% to 37% for the TA coating formed in water for 3 h), which is significant, even if carbon is ubiquitous on surfaces and its quantification by EDS can be affected by instrumental errors up to 1%. The reported values cannot be quantitatively precise because of the limits of EDS in measuring the carbon content. Still, they suggest that the coating is more effective and homogeneous when performed in water than in PBS: higher carbon content (the carbon content rises to 37% when the coating is performed in water and only up to 12% when performed in PBS), lower standard deviation, and better substrate coverage (the magnesium content is reduced to 11% on samples coated in water and 22% on the ones coated in PBS from a starting content of 52%). In agreement with SEM observations, EDS results suggest a submicrometric coating thickness: the EDS penetration depth is close to 1 μm , and the Mg substrate is still detectable after the coating. The higher ability of TA to form a coating on Mg alloy when dissolved in water can be explained by considering the pH of the two solutions: it is 3.5 for the water solution and 6.1 for the PBS one. It can be hypothesized that more Mg^{2+} ions are released into the solution in an acidic environment during the coating procedure. They act as bridges for the formation of tannic acid–magnesium ions complexes at the surface, as reported in the literature [12,14]. The authors have previously observed a similar effect for the Ca^{2+} ions and polyphenols grafting on metallic surfaces [22]. Moreover, a shielding effect due to the possible precipitation of magnesium phosphates from PBS [1] cannot be excluded.

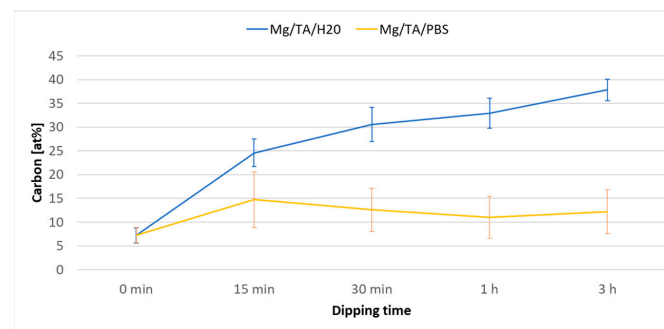


Figure 4. Carbon content (from EDS analyses) on AZ91 samples before and after the TA coating in different conditions.

The EDS analyses on some exemplifying internal surfaces of a structure (denoted as IC, Internal Central, and I, Internal, as shown in Figure 1d) coated in a water tannic acid solution for 3 h evidence a carbon content close to the one observed on the plane samples (30.8% for IC surface and 30.5% for the I surface), suggesting a homogeneous coating of the whole 3D surface, as also supported by the uniform color.

FTIR-ATR spectra of bare and coated samples are reported in Figure 5, compared to the spectrum of tannic acid (TA).

As expected, no significant FTIR peaks can be noticed on bare AZ91 samples. On the other hand, the peaks, characteristic of tannic acid, clearly appear on the coated samples: OH phenolic group (a broad band around 3300 cm^{-1}), C = O (around 1700 cm^{-1}), the vibrations of the benzene ring ($1700\text{--}1400\text{ cm}^{-1}$), the vibration of carboxylic ($1400\text{--}1200\text{ cm}^{-1}$) and C-O groups ($1200\text{--}1000\text{ cm}^{-1}$) [25–27]. FTIR confirms the presence of a coating of tannic acid.

The results of the tape adhesion test are reported in Figure 6; a sample coated for 3 h in a tannic acid water solution was selected and tested.

The tape removes part of the coating during the test. However, a certain portion remains on the magnesium surface, as evidenced by the brownish areas on the sample after the test. The FTIR spectrum of the sample after the tape test (Figure 5) confirms the permanence of a significant amount of tannic acid on the sample surface after the test. Considering that this specific coating is on bioresorbable implants, the need for good mechanical adhesion is mainly restricted to the surgery procedure. In future works, both a specific investigation of the adhesion during simulated implantation and the eventual improvement through a surface pre-treatment will be investigated by the authors.

Fluorescence microscopy (Figure 7) evidences a complete absence of a fluorescent signal on the as-received material, as expected, and the presence of a visible red–orange signal on the coated AZ91 samples, which is particularly evident for the ones coated in the solution of tannic acid in water with an immersion time of 3 h. This effect is due to the polyphenols' auto-fluorescence.

Looking at these results, the selected experimental condition for further experiments is a solution of tannic acid in water and an immersion time of 3 h for forming the coating.

The Folin–Ciocalteu test evidenced a concentration of polyphenols of $0.064 \pm 0.003\text{ mg/ml}$ in gallic acid equivalent for the AZ91 samples coated with tannic acid using dipping for 3 h in a TA solution in water. The result indicates the presence of a significant amount of active tannic acid on the surface of the material, which is more than 1 order of magnitude higher than the one registered on titanium functionalized with natural polyphenols where the presence and activity were evidenced as significant for a biological response [22]. The acid tannic coating's potential antioxidant and anti-inflammatory action here finds first evidence.

Small samples, cut from the AZ91 3D structures, as-received and coated with tannic acid for 3 h in a water solution, were subjected to degradation tests. Each sample was soaked in PBS for up to 14 days and characterized for macro and micro appearances and

chemical composition. In addition, the pH and magnesium content of the soaking solutions were measured at different experimental times. The results are reported in Figure 8.

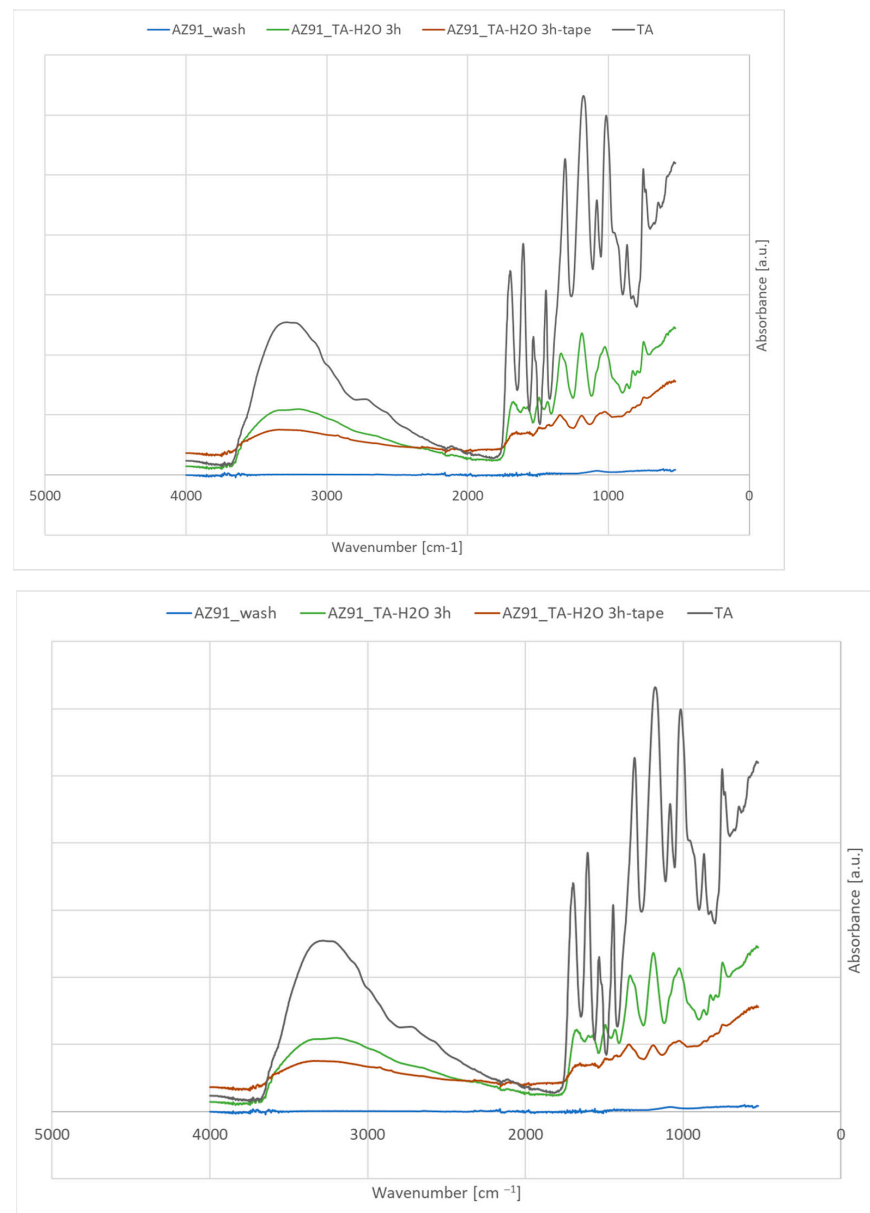


Figure 5. The samples of AZ91 as-received (washed) and coated in optimized conditions (3 h in a tannic acid water solution) were analyzed before and after the tape adhesion test with FTIR-ATR. The spectrum of tannic acid (TA) is reported as a reference.

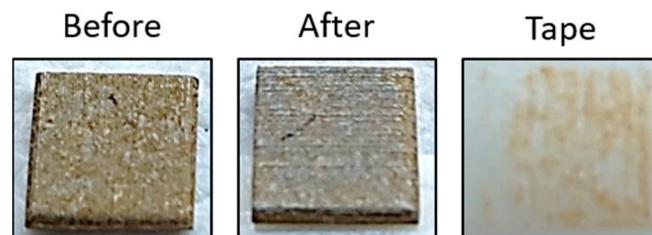


Figure 6. Images of a sample treated for 3 h in a tannic acid water solution before and after the tape adhesion test and the tape used for the test.

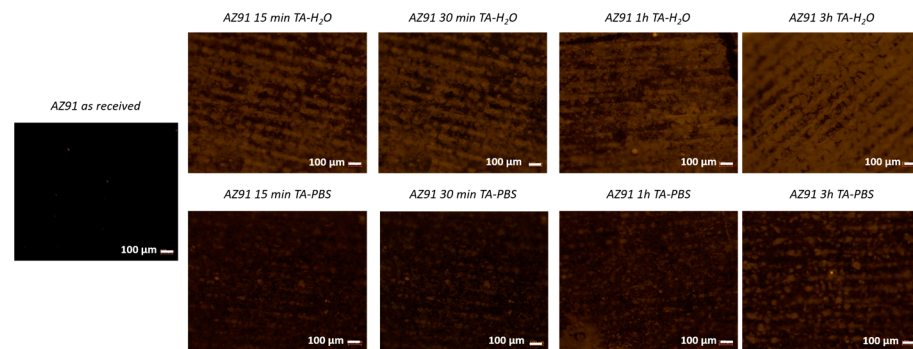


Figure 7. Fluorescence microscopy on AZ91 samples before and after the TA coating in different conditions.

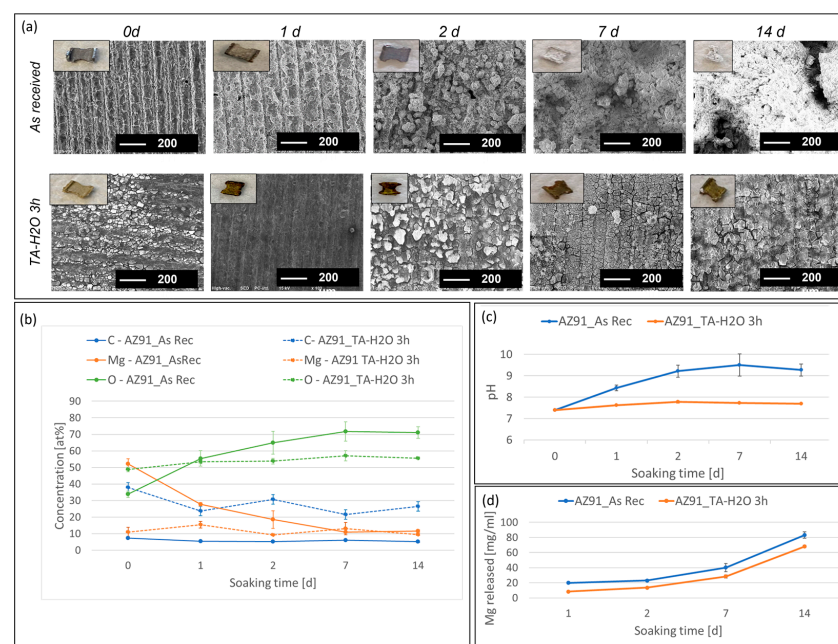


Figure 8. The results of the degradation tests: (a) visual appearance and surface topography from SEM, (b) surface chemical composition from EDS analyses, (c) pH of PBS at different soaking times (*), and (d) Mg concentration in PBS at different soaking times (*). (*) Solution refresh was performed every 3 days; data for 7 and 14 days are related to solutions after the refresh.

It can be observed that the visual appearance of the as-received samples significantly changes after soaking, especially from 7d on, with the reduction of the sample size and the formation of white deposits (Figure 8a). On the other hand, the coated samples are almost unchanged even after 14 days of soaking in PBS. These results are confirmed by weight variations measurements which underline almost unchanged weight for TA coated samples (0.03%, −3.03%, and 0.43% weight variation at 1, 2, and 14 days, respectively) and a more pronounced and variable trend for uncoated ones (−2.73%, −1.04%, and 13.01% weight variation at 1, 2, and 14 days, respectively). Microscopic observations at SEM (Figure 8a) confirm this result, showing a topography close to the one observable in Figure 2 for the coated samples and the appearance of an increasing amount of deposits covering the pristine topography on the as-received ones.

The EDS analyses (Figure 8b) confirm that the surface composition of the coated samples is almost unchanged. At the same time, a significant decrease in the magnesium content and an increase in oxygen can be noticed on the as-received samples after the degradation test. Even if not quantitatively precise because of the limits of EDS, carbon's detected values align with a progressive and incomplete coating release during soaking.

The permanence of the tannic coating, even after a prolonged soaking in PBS, is of great interest for an enhanced biological response.

The pH of PBS used for the degradation tests (Figure 8c) maintains close to the physiological one in the case of the coated samples, while it rises to 8.5 after 1 day and up to 9.5 after 7 days in the case of the as-received samples.

Finally, a particular release of Mg^{2+} ions in PBS can be observed during the degradation test (Figure 8d), and it is significantly higher for the uncoated samples.

All these results suggest that the TA coating obtained by dipping the Mg alloy into a water solution can slow down the degradation of the AZ91 alloy in physiological conditions (PBS solution) and it is at least partially maintained on the surface.

The results show that the tannic acid coating acts as a barrier against dissolution since it homogeneously covers the magnesium alloy surface, protecting it from reacting with the surrounding liquid medium. Comparing the results obtained here with the literature, the efficacy of this simple process without any potentially toxic linker (such as hexamethylenediamine [17]), salt (such as magnesium chloride or sulfate or hexavalent chromium compounds [12,28]), or expensive pre-treatment (such as micro-arc oxidation [16] or multistep treatments to avoid the fast reaction between the reagents [15]) was here proven for the AZ91 alloy. The obtained value of Mg^{2+} ion release at 14 days in PBS is in line (about 40% less than the untreated alloy) with what is reported in the literature for similar coatings obtained by using hexamethylenediamine and gallic acid [17] or tannic acid and magnesium chloride (with a pre-treatment in NaOH) [12]. Furthermore, the pH values of PBS registered after a prolonged soaking of the coated samples are in line, or even lower, compared to those of pre-oxidized samples coated with gallic acid [16]. What is relevant is that a 3D microporous structure was studied in the present paper with an enlarged effective area compared to a bulk sample. The investigated coating here is as effective as more complex ones on bulk samples with a lower surface area. A significant advantage of this process is also no risk of toxicity because of the exposition of amine groups [15,28].

In vivo tests show that it is not easy to realistically mimic the biological degradation process of magnesium alloys by immersion or electrochemical tests [17] because of the difference due, for instance, to the encapsulating granulation tissue, which avoids magnesium hydroxide from falling from the substrate. On the other side, the results of *in vitro* degradation tests must be considered as preliminary values for a first screening of the coatings before *in vitro* biological tests or *in vivo* experiments without the ambition to measure the effective corrosion rate of an implant. The persistence of the coating after soaking in PBS for several days is of great interest considering the proven efficacy of polyphenols for an antioxidative (redox reactivity and scavengers of radical oxygen species) and anti-inflammatory action, as well as a selective action on different cell lines (suppression of fibroblast and smooth muscle cells growth and stimulation of osteoblastic cell proliferation) [16].

4. Conclusions

Due to the proposed combination of innovative manufacturing methods, cast magnesium-based constructs: FDM 3D printing and investment casting can be quickly fabricated on demand and in any shape, e.g., bio-inspired structures. The proposed approach provides the highest level of customization, repeatability, and flexibility for producing biodegradable and bioresorbable bone implants with orifices facilitating tissue ingrowth and regeneration. Tannic acid coatings were successfully obtained on 3D porous structures made of the AZ91 Mg alloy using a dipping procedure in a tannic acid water solution. The process is fast, reproducible, sustainable, and cheap. The coating is homogeneous and thin and completely maintains the metal surface microtopography. The tannic acid coating preserves the AZ91 alloy from rapid degradation in PBS, maintaining the pH close to the physiological one for up to 14 days with a coating and metal surface composition analogous to the one of the unsoaked material.

The proposed technique effectively coats 3D porous structures and does not employ toxic reagents or expensive equipment.

The results of this preliminary study suggest that this coating is promising for controlling the degradation of magnesium alloys for biomedical applications. Further experiments will be focused on an in-depth characterization of corrosion on bare and coated samples, mechanical adhesion of the coating, and cellular response, investigating biocompatibility on specific cells, e.g., osteoblasts, as well as the inflammatory response.

Author Contributions: Conceptualization, S.S., A.D., K.N. and S.F.; methodology, S.S., A.D., K.N. and S.F.; validation, A.D. and S.F.; investigation, A.D. and S.F.; resources, S.S. and K.N.; writing—original draft preparation S.S., A.D., K.N. and S.F.; writing—review and editing, S.S., A.D. and S.F.; supervision, S.S. and S.F.; project administration, S.S. and S.F. All authors have read and agreed to the published version of the manuscript.

Funding: This research received no external funding.

Institutional Review Board Statement: Not applicable.

Informed Consent Statement: Not applicable.

Data Availability Statement: Data will be available upon request.

Acknowledgments: The collaboration was carried out within the European Virtual Institute on Knowledge-based Multifunctional Materials AISBL (KMM-VIN).

Conflicts of Interest: The authors declare no conflict of interest.

References

1. Wang, J.-L.; Xu, J.-K.; Hopkins, C.; Chow, D.H.-K.; Qin, L. Biodegradable Magnesium-Based Implants in Orthopedics—A General Review and Perspectives. *Adv. Sci.* **2020**, *7*, 1902443. [[CrossRef](#)] [[PubMed](#)]
2. Costantino, M.D.; Schuster, A.; Helmholz, H.; Meyer-Rachner, A.; Willumeit-Römer, R.; Luthringer-Feyerabend, B.J.C. Inflammatory response to magnesium-based biodegradable A implant materials. *Acta Biomater.* **2020**, *101*, 598–608. [[CrossRef](#)] [[PubMed](#)]
3. Agarwal, S.; Curtin, J.; Duffy, B.; Jaiswal, S. Biodegradable magnesium alloys for orthopaedic applications: A review on corrosion, biocompatibility and surface modifications. *Mater. Sci. Eng. C* **2016**, *68*, 948–963. [[CrossRef](#)] [[PubMed](#)]
4. Moravej, M.; Mantovani, D. Biodegradable Metals for Cardiovascular Stent Application: Interests and New Opportunities. *Int. J. Mol. Sci.* **2011**, *12*, 4250–4270. [[CrossRef](#)] [[PubMed](#)]
5. Seitz, J.-M.; Eifler, R.; Bach, F.-W.; Maier, H.J. Magnesium degradation products: Effects on tissue and human metabolism. *J. Biomed. Mater. Res. A* **2014**, *102*, 3744–3753. [[CrossRef](#)]
6. Liu, Y.; Zhang, Y.; Wang, Y.-L.; Tian, Y.-Q.; Chen, L.-S. Research progress on surface protective coatings of biomedical degradable magnesium alloys. *J. Alloys Compd.* **2021**, *885*, 161001. [[CrossRef](#)]
7. Hornberger, H.; Virtanen, S.; Boccaccini, A. Biomedical coatings on magnesium alloys—A review. *Acta Biomater.* **2012**, *8*, 2442–2455. [[CrossRef](#)]
8. Shavandi, A.; Bekhit, A.E.-D.A.; Saeedi, P.; Izadifar, Z.; Bekhit, A.A.; Khademhosseini, A. Polyphenol uses in biomaterials engineering. *Biomaterials* **2018**, *167*, 91–106. [[CrossRef](#)]
9. Albuquerque, B.R.; Heleno, S.A.; Oliveira, M.B.P.P.; Barros, L.; Ferreira, I.C.F.R. Phenolic compounds: Current industrial applications, limitations and future challenges. *Food Funct.* **2020**, *2*, 14–29. [[CrossRef](#)]
10. Rahim, A.A.; Kassim, J. Recent Development of Vegetal Tannins in Corrosion Protection of Iron and Steel. *Recent Pat. Mater. Sci.* **2008**, *1*, 223–231. [[CrossRef](#)]
11. Nardeli, J.V.; Fugivara, C.S.; Taryba, M.; Pinto, E.R.P.; Montemor, M.F.; Benedetti, A.V. Tannin: A natural corrosion inhibitor for aluminum alloys. *Prog. Org. Coat.* **2019**, *135*, 368–381. [[CrossRef](#)]
12. Asgari, M.; Yang, Y.; Yang, S.; Yu, Z.; Yarlagadda, P.K.D.V.; Xiao, Y.; Li, Z. Mg–Phenolic Network Strategy for Enhancing Corrosion Resistance and Osteocompatibility of Degradable Magnesium Alloys. *ACS Omega* **2019**, *4*, 21931–21944. [[CrossRef](#)] [[PubMed](#)]
13. Chen, X.; Li, G.; Lian, J.; Jiang, Q. Study of the formation and growth of tannic acid based conversion coating on AZ91D magnesium alloy. *Surf. Coat. Technol.* **2009**, *204*, 736–747. [[CrossRef](#)]
14. Zhang, B.; Yao, R.; Li, L.; Wang, Y.; Luo, R.; Yang, L.; Wang, Y. Green Tea Polyphenol Induced Mg²⁺-rich Multilayer Conversion Coating: Toward Enhanced Corrosion Resistance and Promoted in Situ Endothelialization of AZ31 for Potential Cardiovascular Applications. *ACS Appl. Mater. Interfaces* **2019**, *11*, 41165–41177. [[CrossRef](#)] [[PubMed](#)]
15. Zhang, H.; Shen, X.; Wang, J.; Huang, N.; Luo, R.; Zhang, B.; Wang, Y. Multistep Instead of One-Step: A Versatile and Multifunctional Coating Platform for Biocompatible Corrosion Protection. *ACS Biomater. Sci. Eng.* **2019**, *5*, 6541–6556. [[CrossRef](#)]
16. Lee, H.-P.; Lin, D.-J.; Yeh, M.-L. Phenolic Modified Ceramic Coating on Biodegradable Mg Alloy: The Improved Corrosion Resistance and Osteoblast-Like Cell Activity. *Materials* **2017**, *10*, 696. [[CrossRef](#)]

17. Chen, S.; Zhang, J.; Chen, Y.; Zhao, S.; Chen, M.; Li, X.; Maitz, M.F.; Wang, J.; Huang, N. Application Of Phenol/Amine Copolymerized Film Modified Magnesium Alloys: Anticorrosion And Surface Biofunctionalization. *ACS Appl. Mater. Interfaces* **2015**, *7*, 24510–24522. [[CrossRef](#)]
18. Zhang, H.; Luo, R.; Li, W.; Wang, J.; Maitz, M.F.; Wang, J.; Wan, G.; Chen, Y.; Sun, H.; Jiang, C.; et al. Epigallocatechin gallate (EGCG) induced chemical conversion coatings for corrosion protection of biomedical MgZnMn alloys. *Corros. Sci.* **2015**, *94*, 305–315. [[CrossRef](#)]
19. *ASTM D 3359-97*; Standard Test Methods for Measuring Adhesion by Tape Test. American Society for Testing and Materials: West Conshohocken, PA, USA, 1997.
20. Lavid, N.; Schwartz, A.; Yarden, O.; Tel-Or, E. The involvement of polyphenols and peroxidase activities in heavy-metal accumulation by epidermal glands of the water lily (Nymphaeaceae). *Planta* **2001**, *212*, 323–331. [[CrossRef](#)]
21. Talamond, P.; Verdeil, J.-L.; Conéjéro, G. Secondary metabolite localization by autofluorescence in living plant cells. *Molecules* **2015**, *20*, 5024–5037. [[CrossRef](#)]
22. Riccucci, G.; Cazzola, M.; Ferraris, S.; Gobbo, V.; Guaita, M.; Spriano, S. Surface functionalization of Ti6Al4V with an extract of polyphenols from red grape pomace. *Mater. Des.* **2021**, *206*, 109776. [[CrossRef](#)]
23. Ferraris, S.; Zhang, X.; Prenesti, E.; Corazzari, I.; Turci, F.; Tomatis, M.; Vernè, E. Gallic acid grafting to a ferrimagnetic bioactive glass-ceramic. *J. Non-Cryst. Solids* **2016**, *432*, 167–175. [[CrossRef](#)]
24. *ASTM G31-72*; Standard Practice for Laboratory Immersion Corrosion Testing of Metals. ASTM International: West Conshohocken, PA, USA, 1999.
25. Xu, Z.; Ye, H.; Li, H.; Xu, Y.; Wang, C.; Yin, J.; Zhu, H. Enhanced Lithium Ion Storage Performance of Tannic Acid in LiTFSI Electrolyte. *ACS Omega* **2017**, *2*, 1273–1278. [[CrossRef](#)] [[PubMed](#)]
26. El-damhougy, T.K.; Ahmed, A.S.I.; Gaber, G.A.; Mazied, N.A.; Bassioni, G. Radiation synthesis for a highly sensitive colorimetric hydrogel sensor-based p(AAc/AMPS)-TA for metal ion detection. *Results Mater.* **2021**, *9*, 100169. [[CrossRef](#)]
27. Rajar, K.; Soomro, R.A.; Ibupoto, Z.H.; Sirajuddin; Balouch, A. Tannic acid assisted copper oxide nanoglobules for sensitive electrochemical detection of bisphenol A. *Int. J. Food Prop.* **2017**, *20*, 1359–1367. [[CrossRef](#)]
28. Chen, X.; Li, G.; Lian, J.; Jiang, Q. An organic chromium-free conversion coating on AZ91D magnesium alloy. *Appl. Surf. Sci.* **2008**, *255*, 2322–2328. [[CrossRef](#)]

Disclaimer/Publisher’s Note: The statements, opinions and data contained in all publications are solely those of the individual author(s) and contributor(s) and not of MDPI and/or the editor(s). MDPI and/or the editor(s) disclaim responsibility for any injury to people or property resulting from any ideas, methods, instructions or products referred to in the content.